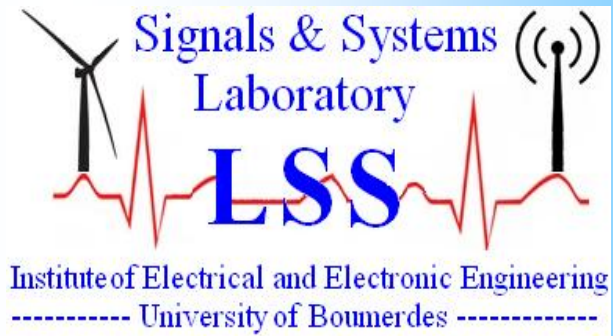


People's Democratic Republic of Algeria
Ministry of Higher Education and Scientific research
M'hamed Bougara University, Boumerdes
Institute of Electrical and Electronic Engineering,
Laboratory of Signals and Systems (LSS)



ALGERIAN JOURNAL OF SIGNALS AND SYSTEMS

ISSN : 2543-3792

Title: Three-phase Three-level Inverter Grid-tied PV System with Fuzzy Logic Control based MPPT

Authors: Yacine AYACHI AMOR^{(1)*}, Farid HAMOUDI⁽¹⁾, Aissa KHELDOUN⁽²⁾

Affiliations:

⁽¹⁾ Laboratoire de Maitrise des Energies Renouvelables (LMER), Faculté de Technologie, Université de Bejaia, 06000 Bejaia, Algeria.

⁽²⁾ Signals and Systems Laboratory, Institute of Electrical and Electronic Engineering, Université M'hamed Bougara de Boumerdes, Avenue of Independence, 35000 Boumerdes, Algeria.

Page range: 96- 105

IMPORTANT NOTICE

This article is a publication of the Algerian journal of Signals and Systems and is protected by the copyright agreement signed by the authors prior to its publication. This copy is sent to the author for non-commercial research and education use, including for instruction at the author's institution, sharing with colleagues and providing to institution administration. Other uses, namely reproduction and distribution, selling copies, or posting to personal, institutional or third party websites are not allowed.

Volume : 3 Issue : 3 (September 2018)

Laboratory of Signals and Systems

Address : IGEE (Ex-INELEC), Boumerdes University, Avenue de l'indépendance, 35000, Boumerdes, Algeria

Phone/Fax : 024 79 57 66

Email : lss@univ-boumerdes.dz ; ajsyssig@gmail.com

©LSS/2018

Three-phase Three-level Inverter Grid-tied PV System with Fuzzy Logic Control based MPPT

Yacine AYACHI AMOR^{(1)*}, Farid HAMOUDI⁽¹⁾, Aissa KHELDOUN⁽²⁾

⁽¹⁾ Laboratoire de Maitrise des Energies Renouvelables (LMER), Faculté de Technologie, Université de Bejaia, 06000 Bejaia, Algeria.

⁽²⁾ Signals and Systems Laboratory, Institute of Electrical and Electronic Engineering, Université M'hamed Bougara de Boumerdes, Avenue of Independence, 35000 Boumerdes, Algeria.
yacineayachiamor@gmail.com

Abstract: This paper presents a three phase single stage grid connected photovoltaic PV system. Maximum power transfer from the solar array to grid is ensured by using fuzzy logic (FL) based maximum power point tracking (MPPT) controller. The proposed MPPT technique provides fast and high performances under variable climate conditions as well as sudden variation of irradiance level. Change of measured photovoltaic power and its rate of change are the input variables of the proposed fuzzy logic controller while the change in reference current is defined as the output variable. In order to meet the power quality required by the international standards, a Space Vector Modulation (SVM) controlled three-level T-type inverter and a series LCL filter are used. To show the effectiveness of the proposed grid-connected system, Matlab/Simulink software is used to carry out the simulation part. Obtained results show the role of each component, particularly the response of the maximum power tracking, the quality of the injected power, the unity power factor operation and the system's efficiency.

Keywords: Fuzzy logic MPPT controller, Three-level T-type inverter, photovoltaic generator, grid connection, power quality

1. INTRODUCTION

Renewable energy coming from natural resources such as the sun is more and more integrating into grid utilities to reduce dependence on conventional power plants. The latter is based on fossil fuels such as coal and oil that sooner or later will run out. Studies estimate that electrical energy use in Algeria will rise to 83 Terawatt-hour (1TWhr = 10^{12} Watts.hour) by 2020 and up to 150 TWhr by 2030, thus the amount of energy being generated by the current power plants pool will not satisfy this demand [1]. To this, some ambitious plans to develop renewable energy sources over the period of 2011-2030 have already started with objective to reach 40% of electricity demand by 2030 from solar and wind [1]. The use of photovoltaic PV systems is considered promising among the various existing of solar energy technologies. This PV system can operate either in standalone mode with the storage system or in grid-tied mode [2]. The grid connected system has the advantage to do not need any storage element that has many economical and technical limitations [3]. The main issues related to the grid-connected systems are maximum power extraction, power quality, overall efficiency, initial investment costs, etc. Single stage grid-connected system has emerged as potential solution that may improve the reliability by reducing the number switching components. This paper investigates the application of fuzzy logic rules to improve the efficiency of maximum power tracking of single stage grid-connected system. The configuration of the latter consists in a T-type inverter being controlled by SVM and LCT filter as interface with grid.

Nowadays, several maximum power point tracking (MPPT) methods are available in literature. Modern MPPTs are either based on Artificial Intelligence or global search algorithms. These methods have shown their effectiveness in terms convergence and time response with respect to conventional ones such as perturb and observe P&O [4] and Hill Climbing (HC) [5]. However, these MPPT methods are very often applied to standalone PV systems where the control variable is the output voltage or the duty cycle the chopper being used. Furthermore, the FLC based maximum power point tracking (MPPT) has been used to control a DC/DC converter for the case of two-stage grid connected architecture [6]-[7]. Single-stage converter allows improving operating efficiency where it is evaluated to be 4 to 10% more than in two-stage systems [8]. This is mainly due to reducing system components and leads to lower cost too. However, as a cost of this simplicity, the control structure becomes more complex [9].

A three phase three-level T-type inverter is used in this study to interface between the PV

generator and the grid. The T-type converters are becoming popular for automotive and photovoltaic (PV) converters to achieve high energy conversion efficiency and better power quality [10]. Compared to the three-level Neutral Point Clamped (NPC) inverter [11], the T-type inverter employs two active bidirectional switches to the DC-link voltage neutral point, which can reduce two clamping diodes per phase leg. Therefore, it provides a lower conduction losses and a smaller size for implementation [12]-[13]. In addition, the simplified Space Vector Pulse Width Modulation (SVPWM) control can be used to achieve the neutral voltage balance based on selecting redundant switching vectors[14] without using additional sensors, as in [15][16].

In this paper, three-phase three-level inverter with MPPT capability for grid interactive PV system is proposed. MPPT is ensured with an intelligent control scheme which is fuzzy logic rules based designed. The fuzzy logic controller (FLC) has high performance under rapidly changing atmospheric conditions. The proposed system covers three-phase, three-level T-type inverter, line frequency transformer to ensure galvanic isolation, LCL output filter to remove high frequency current harmonics, fuzzy logic based MPPT controller and PI current regulator. Proposed MPPT controller defines the reference current value of the inverter and PI regulator shapes the inverter output current. Furthermore, power injected into the grid must have some requirements according to the international standards relating to grid connected systems. Current being injected into the network must be in phase with voltage and have waveform as close to sinusoidal wave as possible so that the THD is less than 5%.

This paper is organized as follows: section 2 presents the description of the systems. Sections 3, 4 and 5 presents respectively PV modeling with MPPT based FLC, inverter modeling based SVM control and LCL filter design. Sections 6 and 7 are devoted simulation results with discussion and conclusion respectively.

2. SYSTEM DESCRIPTION

The detailed block diagram of proposed three-phase grid-tied inverter is given in Fig. 1. As can be seen in the figure, the proposed system consists of the three-level T-type inverter, the line frequency transformer, the phase locked loop (PLL) circuit, the LCL output filter, the fuzzy logic based MPP controller and the PI current controller. The Phase Locked Loop (PLL) is used to provide the synchronization of the inverter output current with the grid voltage. The output of the FLC based MPPT sets the reference for the d-axis current $I_{d,ref}$ hence the active power, and $I_{q,ref}$ is set to be zero in order to achieve the unity power factor operation. These references $I_{d,ref}$ and $I_{q,ref}$ are compared with measured value of $I_{d,meas}$ and $I_{q,meas}$, and the error is processed by PI compensator to generate required V_d and V_q . This latter are transformed back into (abc) coordinates using the inverse Park transformation to get the three-phase voltage reference $U_{ref}(m_a, m_b, m_c)$ of the SVPWM. This latter generates the required pulses to control the three-level inverter and insure the DC voltage balance.

The PI current regulator shapes the inverter output current to remove current error. Proportional and integral gains of the PI regulator are determined by using Ziegler–Nichols method. The LCL filter is used to reduce the output current THD level preferred, line frequency transformer is employed to step up the inverter output voltage to grid voltage level and to obtain galvanic isolation.

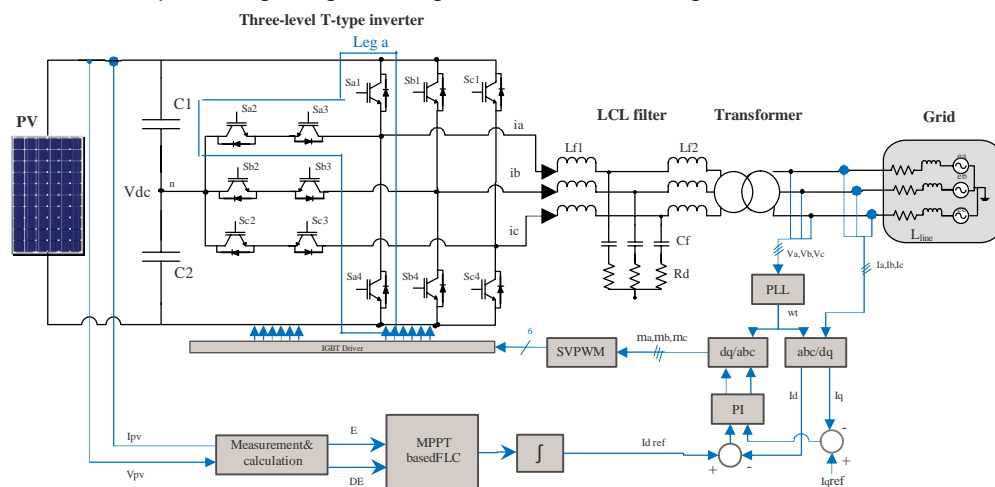


Fig. 1 Block diagram of the proposed system.

3. PV GENERATOR AND MPPT FUZZY LOGIC CONTROLLER

The most common model used to predict energy production in photovoltaic cells is the single diode lumped circuit model, which is derived from physical principles, as depicted in Fig. 2. In this model, the PV cell is usually represented by an equivalent circuit composed of a light-generated current source, a single diode representing the nonlinear impedance of the P-N junction, and series and parallel intrinsic resistances accounting for resistive losses [17].

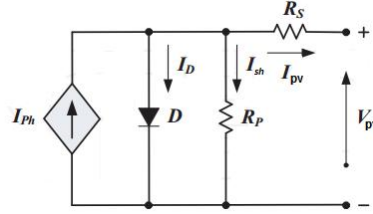


Fig. 2 Electrical equivalent circuit of PV cell.

The mathematical model that predicts the power production of the PV cell becomes an algebraically simply model, being the current-voltage relationship defined in Eq. (1).

$$I_{pv} = I_{ph} - I_s \left[e^{\left(\frac{V_{pv} + I_{pv} R_s}{V_t} \right)} - 1 \right] - \frac{V_{pv} + I_{pv} R_s}{R_p} \quad (1)$$

Where:

I_{pv} : PV cell output current, A.

V_{pv} : PV cell output voltage, V.

I_{ph} : solar cell photocurrent, A.

I_s : The reverse saturation or leakage current of the diode, A.

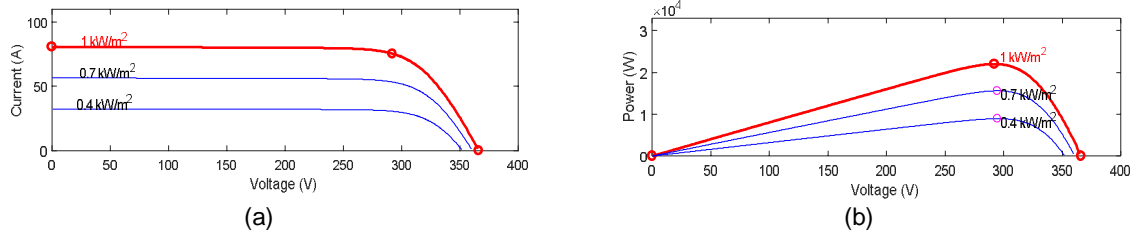


Fig. 3 I-V characteristic (a), P-V characteristic (b) under different irradiance conditions.

The PV cells are grouped in larger units called PV modules which are further interconnected in series-parallel configuration to form PV arrays or PV generators.

The most important issue on a PV system is to get high efficiency from the PV cells, however due to the financial restrictions, the efficiency of a PV panel stays between 9% and 20% in most of the applications. Besides, the PV arrays generate electricity depending on the atmospheric conditions. The I-V curve given in Fig. 3(a) is nonlinear and mainly influenced by solar irradiance variations. In addition, as can be noticed in Fig. 3(b), only the operation point on the knee provides the maximum power, therefore it is important to make the PV generator operates at this point.

In the literature [18] various techniques have been reported to obtain the MPP of a PV system. A fast and accurate MPPT technique based on fuzzy logic has been used in this study. This command offering the advantage of being robust, simple to integrate, and does not require cognition of the exact system modeling.

The Fuzzy logic controller uses the fuzzy logics to make the decisions and to control the output of the controller. The main components in fuzzy logic based MPPT controller are fuzzification, rule-base, inference and defuzzification as illustrated in Fig. 4.

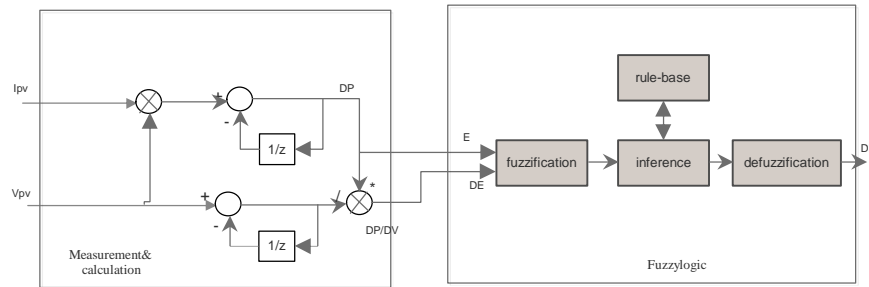


Fig. 4 Structure of FLC.

The fuzzy controller has two input variable namely the power error (E) and its rate of change (DE) and is expressed as,

$$E = P(k) - P(k-1) \quad (2)$$

$$DE = \frac{P(k) - P(k-1)}{V(k) - V(k-1)} \quad (3)$$

Where $P(k)$ and $V(k)$ represents the power and voltage of the PV array at 'k'th instant respectively, E is the power error and DE is the rate of change of power error with respect to the voltage.

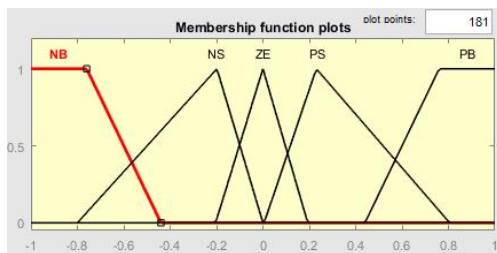


Fig. 5 Membership functions for input variables E and DE.

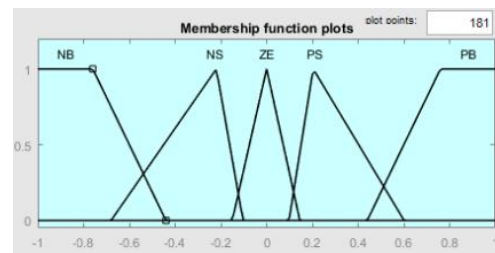


Fig. 6 Membership functions for output variables "change of I_{ref} ".

The three variables of the FLC, the change in PV power, the rate of change in PV power and the change in inverter reference current, have five triangle membership functions for each. The basic fuzzy sets of membership functions for the variables are as shown in Figs. 5 and 6. The fuzzy variables are expressed by linguistic variables 'positive large (PL)', 'positive small (PS)', 'zero error (ZE)', 'negative small (NS)', 'negative large (NL)', for all three variables.

The rule base adjusts the reference current of the T-type inverter based upon the changes in the input of the FLC. The number of rules can be set as desired. The rule base includes 25 rules, which are based upon the five membership functions of the input variables. Table 1 shows the rule base for the FLC.

Table 1 Rule base of FLC.

DE \ E	NB	NS	ZE	PS	PB
NB	NB	NB	ZE	NB	NS
NS	NB	NS	ZE	NS	NS
ZE	ZE	ZE	ZE	ZE	ZE
PS	PB	PS	ZE	PS	PS
PB	PB	PB	ZE	PB	PS

4. THREE-LEVEL T-TYPE INVERTER BASED SVM CONTROL

In this work a three level T-type inverter is selected to interface between the PV generator and the grid, the T-type has proved itself as a high efficiency system compared to the three level NPC where the clamping diodes reduces the necessary diodes from 18 to 12. Furthermore, the reduction of the additional isolated gate drive supplies from six to one is a clear improvement and can drive the costs down [10].

The three-level T-type inverter structure in Fig. 1 shows that each leg contains four active switches S1 to S4 with their antiparallel diodes (free-wheeling diodes), resembling the shape of the rotated character "T". The capacitors C1 and C2 at the DC side are used to split the DC input into two and provide the neutral point O. A positive voltage level $+V_{dc}/2$ (P) is performed by turning on the switches S1 and S2, S2 and S3 for the neutral (O) and S3 and S4 for the negative voltage level $-V_{dc}/2$ (N).

Table 2 Switching states for a three-phase three-level T-type inverter.

Switching states	Status of switching devices (x= a, b, c)				Terminal voltage
	Sx1	Sx2	Sx3	Sx4	
P	ON	ON	OFF	OFF	$V_{dc}/2$
O	OFF	ON	ON	OFF	0
N	OFF	OFF	ON	ON	$-V_{dc}/2$

Different modulation schemes exist for modulating DC-AC multilevel inverters [19]. The Space Vector Pulse Width Modulation (SVPWM) is one of most promising modulation techniques; this method depends on calculating dwell times and selecting promising switching states and sequences. Therefore, it provides flexibility in generating gating signals. Moreover, SVPWM offers 15% modulation range more compared to that of sinusoidal PWM [12]. Considering the availability of modern digital signal processors, SVPWM method is used to enable a better performance for multilevel inverters [21]. Different control objectives are achieved with proper design of SVPWM such as neutral point voltage balance, common-mode voltage reduction, power losses reduction, and fault tolerant control [22].

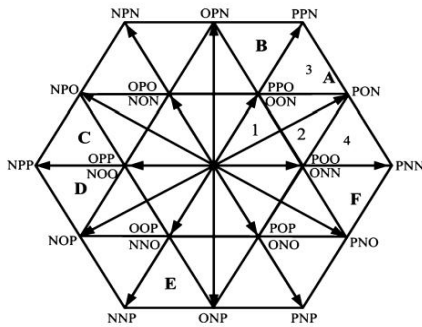


Fig. 7 Space-vector diagram of the three-level converter.

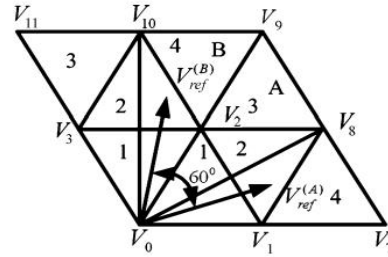


Fig. 8 Two vectors with 60° shifting in the sector A and B.

Each phase leg in the T-type three-level inverter can take one of three possible states: [P], [O], [N]. Table 2 illustrates switch combinations for obtaining these states. Fig. 7 shows the SVPWM diagram for all regions with three level inverter. When the V_{ref} located in the first sector as shown in Fig. 8, the nearest three vectors (V_1 , V_2 and V_8) are used for synthesizing reference vector. The dwell time are calculated as follows:

$$\begin{cases} \vec{V}_{ref} T_s = \vec{V}_1 t_a + \vec{V}_8 t_b + \vec{V}_2 t_c \\ T_s = t_a + t_b + t_c \end{cases} \quad (4)$$

Where; \vec{V}_{ref} is the instantaneous voltage in the α, β frame using Clark's transformation, where being defined by a magnitude and angle as follows: $|\vec{V}_{ref}| = \sqrt{V_\alpha^2 + V_\beta^2}$, $\theta = \tan^{-1}(V_\beta/V_\alpha)$; T_s is the sampling period; t_a , t_b and t_c are the On-time during T_s for voltage vectors V_1 , V_8 and V_2 , respectively.

Using the same procedure, the dwelling time in other regions of sector A can be computed. After calculating the on time, the switching sequence has to be determined. As the converter has some redundant switching states, the switching sequence are arranged in order to achieve low Total Harmonic Distortion (THD) and balancing voltages across the DC-link capacitors.

The switching sequences in the regions of sector (A) are arranged as follows:

Region 1: PPO-POO-OOO-ONN and return.

Region 2: PPO-POO-PON-ONN-ONN and return.

Region 3: PPO-PPN-PON-ONN and return.

Region 4: POO-PON-PNN-ONN and return.

Due to the geometrical symmetry of six sectors, there exists close relationships between on time calculations and on time arrangement for switches of the inverter. Therefore, this symmetry can be extended to the remaining sector based on single computation being done for the first sector only [14].

For example, suppose reference vector A is located in region 2 of sector A, while reference vector B is obtained by rotating vector A counterclockwise by 60° as shown in Fig. 8.

Therefore, the reference vector V_{ref}^B can be expressed in the following form:

$$V_{ref}^B = V_{ref}^A * e^{\frac{j\pi}{3}} = 2/3(-U_b - U_c e^{\frac{j2\pi}{3}} - U_a e^{\frac{-j2\pi}{3}}) \quad (5)$$

When the reference vector is in the other sectors, it will be rotated to sector A by $n\pi/3$ where ($n=1, 2, 3, 4, 5$).

5. LCL FILTER DESIGN

In the grid-connected inverter, a filter is needed as the interface between the inverter and the power grid. Compared with the L filter, the LCL filter is considered to be a preferred choice due to its advantages such as the ability to operate at lower switching frequency, better attenuation, lower current ripple in the current injected to the grid, and reduced cost and size due to relatively small inductor values [23]. To achieve high-quality grid current, the LCL filter should be properly designed. Several characteristics must be taken into consideration in the filter design, such as current ripple, filter size and switching ripple attenuation. Thus, the following parameters are needed for the design: nominal output power (S_n), line to line RMS voltage (U_n) (inverter output voltage), grid frequency (f_g), switching frequency (f_s) and resonance frequency (f_{res}). Similar criteria are required for inductor and capacitor values. Normalized values will help to explain these criteria that are given in Table 3 [24].

Table 3 Normalized values of LCL filter.

Quantity	I_b	Z_b	L_b	C_b
Value	$\frac{S_n}{U_n}$	$\frac{U_n^2}{S_n} = \frac{U_n}{I_b}$	$\frac{L_b}{Z_b}$	$\frac{1}{2\pi f_g Z_b}$

Since the capacitor filter C_f decreases the power factor and unity power factor is desired in grid interactive inverter application [25], the capacitor value of the filter is usually limited to:

$$C_f = 0.05 C_b \quad (6)$$

Higher DC voltage level will result in higher switching losses. So, total value of the inductance must be lower than the 10% of L_b [26]. The difference between L_{f1} and L_{f2} values can be selected for a unique value of the total inductance, L_{f1}/L_{f2} ratio is related to the maximum allowed value of the current ripple at the inverter and the grid side. Therefore, $L_{f1} = L_{f2}$.

An important parameter of the filter is its resonant frequency. The resonance frequency of the LCL filter is related to the values of filter components and is given by the following equation:

$$f_{res} = \frac{1}{2\pi} \sqrt{\frac{L_{f1} + L_{f2}}{L_{f1} L_{f2} C_f}} \quad (7)$$

The resonant frequency must be much higher than the grid frequency while at least one half of the inverter switching frequency. Thus:

$$10f_g \leq f_{res} \leq f_s/2 \quad (8)$$

Finally, the design of the damping resistance comes as the last step. In order to reduce oscillations and unstable states of the filter, a resistor should be added in series with the capacitor filter. This solution is sometimes called 'passive damping' [27]. It is simple and reliable, but it increases the heat losses. The value of the damping resistor can be calculated as:

$$R_d = \frac{1}{3\omega_{res}C_f} \quad (9)$$

6. SIMULATION RESULTS AND DISCUSSION

This section presents the simulation results of the proposed system. Computer simulation has been carried out using MATLAB/Simulink software by using Fuzzy Logic Toolbox.

The PV generator consists of 100 panels of SolarWorld SW220 being connected 10 in series and 10 in parallel. The PV solar farm provides 22KW of nominal maximum power and 292 V of nominal DC voltage at standard test condition STC (irradiation of 1 kW/m² and ambient temperature of 25 C°). The three-phase three-level T-type inverter configured using MOSFET's where the desired pulses provided by the Simplified SVPWM algorithm being coded using M-file. LCL filter is designed using three-phase branches. A block of three-phase transformer steps up the inverter output voltage to match the grid voltage. A grid utility emulated using a three-phase voltage source in series with RL branch. Maximum power point of the PV system is tracked with FLC.

Parameters of components constituting system are given in Table 4.

Table 4 Simulation parameters.

Grid line to line voltage RMS	707 V / 50Hz
Nbr of panels	100 (SolarWorld SW220)
Total PV output power (P)	22KW at (25 C°; 1000 W/m ²)
V _{dc} nominal	292V _{dc}
DC link capacitors C ₁ & C ₂	15.5*10 ⁻³ F
Filter inductors L _{f1} & L _{f2}	5.013*10 ⁻⁴ H
Capacitor Filter C _f	1.77*10 ⁻⁴ F
Damping resistor R _d	0.21 Ω
Current controller PI	K _{IP} =0.8 ; K _{II} =40
Switching frequency (f _s)	5 KHz

In order to test the MPPT controller performance, a sudden change in the irradiance level is used. A 0.8-s period for the decreasing and increasing instantly of irradiance was selected. This irradiation profile starts from 1000 W/m², decreases down to 700 W/m² at t=0.2-s then down to 400 W/m² at t=0.4-s and increases again back to 1000W/m² at t=0.6-s. The temperature is considered constant at 25 C° during the whole simulation process. Solar irradiation level, PV power and input DC voltage are given in Fig. 9.

As we can see from the Fig. 9 the proposed fuzzy logic based MPPT controller has fast transient response. Also, it is clear that fuzzy logic based MPPT controller determines the reference current quickly and PI regulator shapes the current with respect to irradiance level and as a result changes the inverter output current as illustrated in Fig. 10. Also, inverter output current is in sinusoidal waveform and in phase with voltage as shown in Fig. 12.

Fig.11 depicts the output line to line voltage of three level T-type inverter before and after LCL filter. As we can see the wave form is well smoothed. It can be noticed that there is slight shift between the different voltage levels and their fundamental component, that's because LCL filter has shifting properties upon signals filtered.

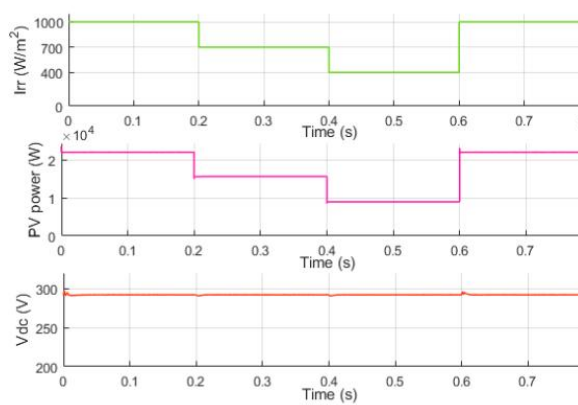


Fig. 9 Irradiance level (upper) ; output PV power (middle); output PV voltage (lower).

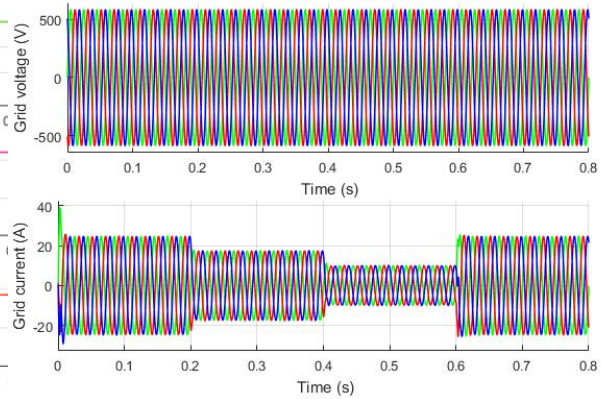


Fig. 10 Output three-phase inverter voltage (upper) and current (lower) after step-up transformer.

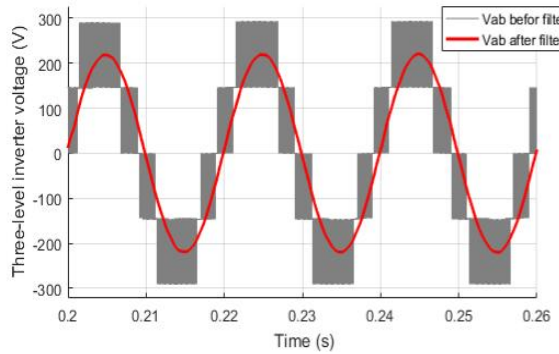


Fig. 11 Output inverter voltage before and after LCL filter.

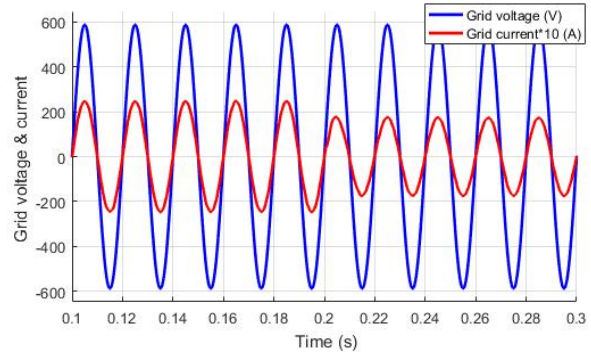


Fig. 12 Grid voltage and current at unity power factor (the current scaled by gain of 10).

From Figs. 13 and 14, we can see that the system efficiently tracks the maximum power at unity power factor with total system efficiency $\eta = 90\%$ at steady state, where $\eta = \frac{P_{out}}{P_{in}} * 100\%$.

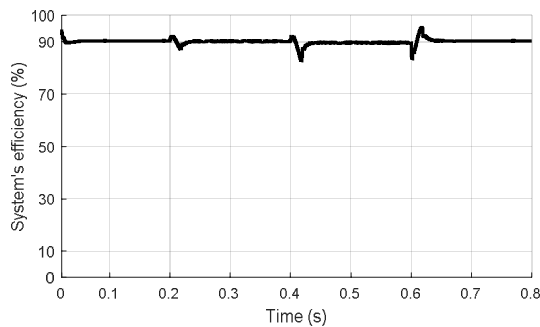


Fig. 13 Efficiency of the whole system.

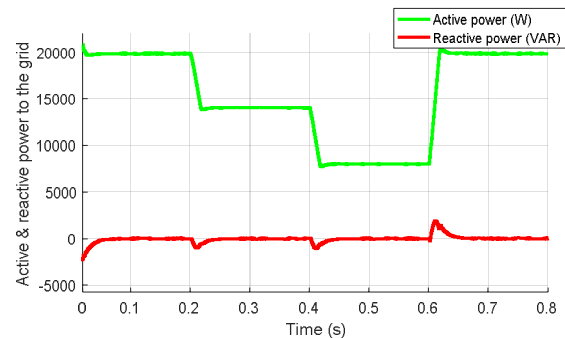


Fig. 14 Injected active and reactive power to the grid.

As can be seen in the Fig. 15 the voltage balance between the upper and lower DC link capacitors (V_{c1} and V_{c2}) have been achieved without using another control loop or additional sensors.

Furthermore, FFT analysis of the inverter output current is given in Fig. 16. As seen from this figure total harmonic distortion level of this current is in the limits of international standards such as IEEE1547 ($0.97\% < 5\%$).

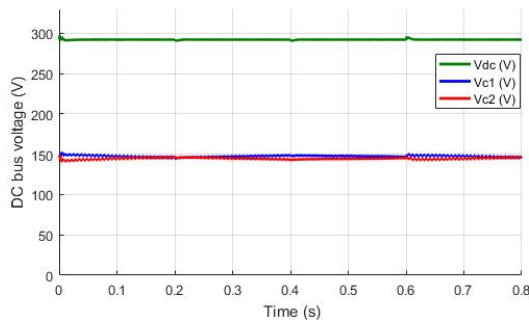


Fig. 15 The voltage balance across the DC-link capacitors of the inverter.

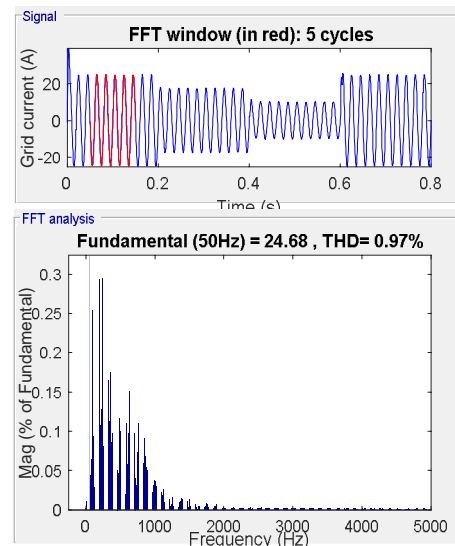


Fig. 16 FFT analysis of the inverter output current (THD=0.97%).

7. CONCLUSION

In this work a three-phase single-stage grid-tied inverter with maximum power point tracking based fuzzy logic controller capability is analyzed, designed and simulated. The goal of our work was to extract the maximum power from the panel, convert it to AC power then inject it into the utility grid. The power quality is insured by using three-level T-type inverter with space vector modulation (SVM) technique in series with LCL filter. The reference current of the inverter is set by proposed MPPT in order to draw the possible highest power from PVs all the time. It seems from the simulation results that the fuzzy logic based MPPT method tracks maximum power point of the PV generator with fast transient response in case of sudden variation in the irradiance level. Also, inverter output current is almost sinusoidal waveform so that, the THD level is below the limits of the international standards ($0.97\% < 5\%$) and unity power factor operation is obtained. Since only one inverter is used for all of the procedures such as grid interactive operation and MPPT, the size and the cost of the system are decreased and total efficiency is increased where it measured as 90%.

References

- [1] A. Zino, "Renewable Energies in Algeria", Arab Climate Resilience initiative: Climate Change Impacts in the Arab Region "Towards Sustainable Energy: Resources, Challenges and Opportunities", Manama, Bahrain, 06-07 October, 2010.
- [2] Hill CA, Such MC, Chen D, Gonzalez J, Grady WM. Battery energy storage for enabling integration of distributed solar power generation. IEEE Transactions on the smart grid. 2012 Jun;3(2):850-7.
- [3] Debnath D, Chatterjee K. Two-stage solar photovoltaic-based stand-alone scheme having battery as energy storage element for rural deployment. IEEE Transactions on Industrial Electronics. 2015 Jul;62(7):4148-57.
- [4] Ishaque K, Salam Z, Lauss G. The performance of perturb and observe and incremental conductance maximum power point tracking method under dynamic weather conditions. Appl Energy 2014;119:228–36. <http://dx.doi.org/10.1016/j.apenergy.2013.12.054.7>
- [5] Kjær SB. Evaluation of the hill climbing and the incremental conductance maximum power point trackers for photovoltaic power systems. IEEE Trans Energy Convers 2012;27:922–9. <http://dx.doi.org/10.1109/TEC.2012.2218816>.
- [6] P. Jose, P. R. Jose "Grid Connected Photovoltaic System with Fuzzy Logic Control Based MPPT" International Journal of Engineering and Innovative Technology (IJEIT) Vol. 3, Issue 8, February 2014.

- [7] D. Reddy, S. Ramasamy "A fuzzy logic MPPT controller based three phase grid-tied solar PV system with improved CPI voltage" International Conference on Innovations in Power and Advanced Computing Technologies [i-PACT 2017].
- [8] H. Patel,, V. Agarwal, MPPT scheme for a PV-fed single-phase single-stage grid-connected inverter operating in CCM with only one current sensor, IEEE Trans. Energy Convers. 24(1) (2009) 256–63. 10.1109/TEC.2008.2005282.
- [9] R. Kadri,, J.-P. Gaubert,, G. Champenois, An Improved Maximum Power Point Tracking for Photovoltaic Grid-Connected Inverter Based on Voltage-Oriented Control, IEEE Trans. Ind. Electron. 58(1) (2011) 66–75. 10.1109/ICMA.2013.6617987.
- [10] M. Schweizer,, S. Member,, J.W. Kolar, Design and Implementation of a Highly Efficient Three-Level T-Type Converter for Low-Voltage Applications, IEEE Trans. Power Electron. 28(2) (2013) 899–907.
- [11] A.A. Noureddine, A.A. Yacine,, K. Aissa,, M. Brahim, Comprehensive modeling and simulation of grid-tied PV system, in: 5th International Conference on Electrical Engineering - Boumerdes (ICEE-B), Boumerdes, Algeria., 2017, pp. 1–6. [10.1109/ICEE-B.2017.8191994](#)
- [12] A. Zorig,, M. Belkheiri,, S. Barkat, Control of three-level T-type inverter based grid connected PV system, in: 2016 13th International Multi-Conference on Systems, Signals & Devices (SSD), 2016, pp. 66–71.
- [13] M. Aly,, G.M. Dousoky,, S. Masahito, Design and validation of SVPWM algorithm for thermal protection of T-type three-level inverters, in: IEEE International Telecommunications Energy Conference (INTELEC), 2015.
- [14] H. Hu, W. Yao,, Z. Lu, Design and implementation of three-level space vector PWM IP core for FPGAs, IEEE Trans. Power Electron. 22(6) (2007) 2234–44. 10.1109/TPEL.2007.909296.
- [15] S. Ozdemir,, N. Altin,, I. Sefa, Single stage three level grid interactive MPPT inverter for PV systems, Energy Convers. Manag. 80 (2014) 561–72. 10.1016/j.enconman.2014.01.048.
- [16] A. Zorig,, M. Belkheiri,, S. Barkat, Control of three-level NPC inverter based grid connected PV system, in: 3rd International Conference on Control, Engineering & Information Technology (CEIT), Tlemcen, Algeria, 2015, pp. 66–71.
- [17] King, D.L.; Kratochvil, J.A.; Boyson, W.E. and Bower, W.I. Field Experience with a New Performance Characterization Procedure for Photovoltaic Arrays. In: 2nd World Conference on Photovoltaic Solar Energy Conversion; 1998. P. 6-10.
- [18] Y. Bouzelata, E. Kurtb, N. Altin, R. Chenni "Design and simulation of a solar supplied multifunctional active power filter and a comparative study on the current-detection algorithms" Renewable and Sustainable Energy Reviews Vol. 43, March 2015, Pages 1114-1126.
- [19] S. Calligaro, F. Pasut, R. Petrella, and A. Pevere, "Modulation techniques for three-phase three-level NPC inverters: A review and a novel solution for switching losses reduction and optimal neutral-point balancing in photovoltaic application", in Proc. IEEE APEC'13, pp. 2997-3004.
- [20] S. de Pablo,, A.B. Rey,, L.C. Herrero,, J.M. Ruiz, A simpler and faster method for SVM implementation, Power Electron. Appl. 2007 Eur. Conf. (1) (2007) 1–9. 10.1109/EPE.2007.4417751.
- [21] A.A. Yacine,, A.A. Noureddine,, K. Aissa,, M. Brahim, Design and Implementation of Three-Level Inverter for Grid-tied PV Systems, in: 5th International Conference on Electrical Engineering - Boumerdes (ICEE-B), Boumerdes, Algeria., 2017, pp. 0–5.
- [22] C. Charumit, and V. Kinnarees, "Discontinuous SVPWM techniques of three-leg VSI-fed balanced two-phase loads for reduced switching losses and current ripple", IEEE Trans. Power Electron., vol. 30, no. 4, pp 2191-2204, Apr. 2015.
- [23] D. Pan, X. Ruan, C. Bao, W. Li, and X. Wang, "Capacitor-current- feedback active damping with reduced computation delay for improving robustness of LCL-type grid-connected inverter," IEEE Trans. Power Electron, vol. 29, no. 7, pp. 3414-3427, Jul. 2014.
- [24] Liserre M, Blaabjerg F, Hansen S. Design and control of an LCL-filter-based three-phase active rectifier. IEEE Trans Ind Appl 2005;41(5):1281–91.
- [25] M.A.E. Alali,, J.-P. Barbot, A First Order Sliding Mode Controller for Grid Connected Shunt Active Filter with a LCL Filter, IFAC-PapersOnLine 50(1) (2017) 14812–7.
- [26] Raoufi M, Lamchich TM. Average current mode control of a voltage source inverter connected to the grid: application to different filter cells. J Electr Eng 2004;55(3-4):77–82.10.1016/j.ifacol.2017.08.2563.
- [27] M. Ben Saïd-Romdhane,, M.W. Naouar,, I.S. Belkhodja,, E. Monmasson, Simple and systematic LCL filter design for three-phase grid-connected power converters, Math. Comput. Simul. 130 (2016) 181–93. 10.1016/j.matcom.2015.09.011.